Resource

Cell Chemical Biology

Live-cell imaging to analyze intracellular aggregation of recombinant IgG in CHO cells

Graphical abstract

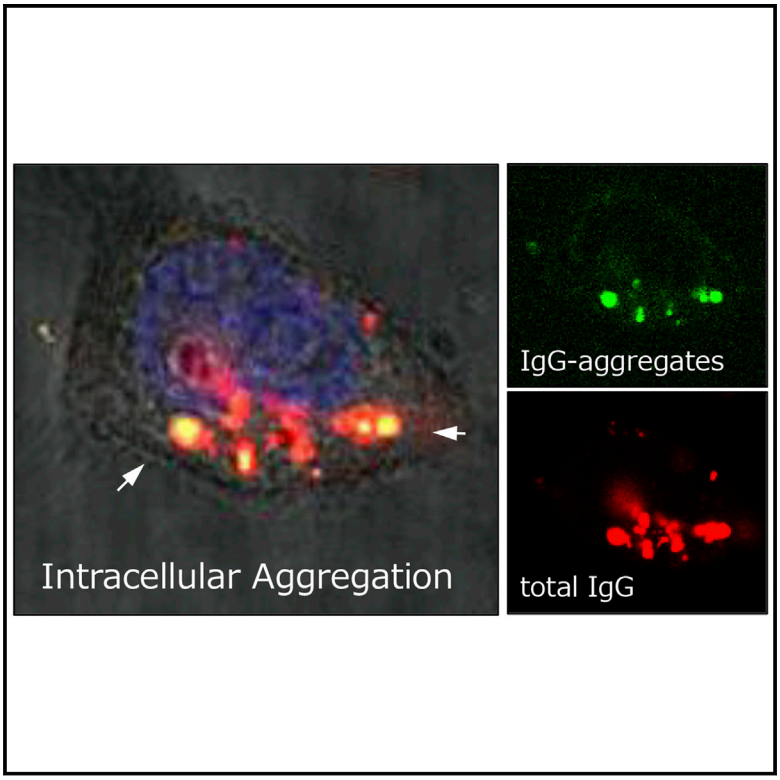

Authors

Yukako Senga, Motomichi Doi, Masayoshi Onitsuka, Shinya Honda

Correspondence

s.honda@aist.go.jp

In brief

Senga et al. develop a method for monitoring intracellular IgG aggregates in antibody-producing CHO cells using the artificial small protein, AF.2A1. This method can be used to minimize protein aggregation right from the early steps of production of therapeutic antibodies with high yield/quality.

Highlights

- A method to detect intracellular non-native antibody aggregates was established
- The formation, dynamics, and degradation of intracellular aggregates was visualized
- Correlation between intra- and extracellular aggregates suggests direct secretion
- This work represents progress toward high-quality production of therapeutic antibodies by aggregate minimization

Senga et al., 2022, Cell Chemical Biology *29*, 120–132
January 20, 2022
https://doi.org/10.1016/j.chembiol.2021.08.010

CellPress

CellPress
OPEN ACCESS

Cell Chemical Biology

Resource

Live-cell imaging to analyze intracellular aggregation of recombinant IgG in CHO cells

Yukako Senga,[1] Motomichi Doi,[1] Masayoshi Onitsuka,[2] and Shinya Honda[1,3,*]
[1]Biomedical Research Institute, National Institute of Advanced Industrial Science and Technology (AIST), Higashi, Tsukuba, Ibaraki 305-8566, Japan
[2]Graduate School of Technology, Industrial and Social Sciences, Tokushima University, 2-1 Minamijosanjima, Tokushima, Tokushima 770-8513, Japan
[3]Lead contact
*Correspondence: s.honda@aist.go.jp
https://doi.org/10.1016/j.chembiol.2021.08.010

SUMMARY

Recombinant immunoglobulin G (IgG) aggregates are formed during their production. However, the process underlying intracellular/extracellular aggregation in cell culture conditions is not well understood, and no effective method exists to assess IgG aggregates. Here, we establish an approach to detect intracellular aggregates using AF.2A1, a small artificial protein that binds to non-native IgG conformers and aggregates. Fluorescent-labeled AF.2A1 is prepared via conjugation and transfected into antibody-producing Chinese hamster ovary (CHO) cells. Micrographic images show intracellular IgG aggregates in CHO cells. The relative amount of intracellular aggregates (versus total intracellular IgG) differed depending on the type of additives used during cell culture. Interestingly, the relative amount of intracellular aggregates moderately correlates with that of *in vitro* extracellular IgG aggregates, suggesting they are secreted. This method will allow the investigation of antibody aggregation in cells, and may guide the production of therapeutic antibodies with high yield/quality.

INTRODUCTION

Biopharmaceuticals for the treatment of serious diseases, such as allergy, cancers, and autoimmune diseases, should be of high quality to ensure efficacy and safety in their medical use (Food and Drug Administration, 2014). In particular, a therapeutic antibody should be soluble and stable at high protein concentration. However, as immunoglobulin G (IgG) is a fragile large macromolecule, it is prone to degradation and/or aggregation during the different steps of the manufacturing process (e.g., cell culture, purification, and formulation). Such fragments and/or aggregates also emerge during delivery and storage. Antibody aggregates can induce immunogenic reactions and complications, affecting the efficacy and safety of the product (Cromwell et al., 2006). Of note, immunogenicity, here, refers to the generation of anti-drug antibodies in the patient's body after administration (Food and Drug Administration, 2014; European Medicines Agency, 2015). Hence, the appropriate assessment of antibody aggregates is essential for the development and production of safe therapeutic antibodies.

IgG molecules form different types of aggregates when exposed to stress-inducing factors such as acidic pH and agitation (Imamura and Honda, 2016; Joubert et al., 2011; Senga and Honda, 2018; Senga et al., 2017). Thus, these aggregates need to be evaluated using a variety of analysis methods. Size exclusion chromatography (SEC), static light scattering (SLS)/dynamic light scattering (DLS), and atomic force microscopy (AFM) are well suited for analyzing smaller, nanometer-sized aggregates (Den Engelsman et al., 2011; Imamura and Honda, 2016), whereas scanning electron microscopy (SEM) and transmission electron microscopy (TEM) can be used to evaluate aggregates of various sizes (from nanometer- to micrometer-sized aggregates) (Arosio et al., 2012). Flow imaging (FI) and light obscuration (LO) are used for larger, micrometer-sized aggregates (Den Engelsman et al., 2011). In addition, manufacturers often use other methods, such as analytical ultracentrifugation (AUC), field flow fractionation (FFF), nano tracking analysis (NTA), and resonant mass measurement (RMM) (Den Engelsman et al., 2011; Patel et al., 2012). Using these methods, the aggregation mechanism of IgG molecules has been investigated extensively under conditions mimicking the manufacturing stages, including the purification, formulation, transportation, and storage (Imamura and Honda, 2016; Senga et al., 2019). However, despite the availability of so many methods, only a few are available to selectively assess IgG aggregates during cell culture and little is known about the intracellular aggregation mechanism.

Therapeutic antibodies are mostly manufactured using Chinese hamster ovary (CHO) cells, one of the most common industrial mammalian cell lines (Kunert and Reinhart, 2016). In CHO cells, in addition to recombinant IgG, various intrinsic proteins (so-called host cell proteins) and other macromolecules are present in condensed forms. Therefore, it is difficult to selectively analyze intracellular aggregates in living cells; the above-mentioned biophysical methods generally require an abundant sample with

high purity. Moreover, direct evaluation of the extracellular aggregates present in culture medium using conventional methods is difficult; of note, the culture medium also contains secretory substances from CHO cells. To overcome these challenges, Paul et al. (2015) recently attempted to evaluate aggregates in culture supernatants using fluorescent dyes.

In general, a recombinant protein expressed in mammalian cells is post-translationally modified to form the most stable native conformation and secreted via the ER quality control mechanism (Ellgaard et al., 1999; Feige et al., 2010). When misfolded non-native conformers are generated in the cells, they are usually degraded via the intracellular quality control mechanism (Lippincott-Schwartz et al., 1988; Vembar and Brodsky, 2009). However, in the case of antibodies, it is not clear whether IgG aggregates are formed intracellularly or extracellularly during culture. As per the practical experience, the production of a recombinant IgG using CHO cells yields IgG aggregates (1.6%–3.6% over 4–12 days) in cell culture supernatants (Cromwell et al., 2006). Assuming the intracellular quality control mechanism of antibody-producing CHO cells is effective, the presence of IgG aggregates in supernatants suggests the extracellular formation of IgG aggregates. However, Onitsuka et al. (2019) recently obtained indirect evidence suggesting the intracellular formation of IgG aggregates in CHO cells and their secretion.

Although the emergence of aggregates remains unclear, several relevant findings have been reported. The amount of IgG aggregates found in supernatants varies depending on the amino acid sequence of the antibody, cell line characteristics, clonal variation, as well as the cell culture media and culture conditions (Dengl et al., 2013; Gomez et al., 2012; Jing et al., 2012; Onitsuka et al., 2014). Importantly, the aggregates can be classified into different types with respect to solubility, covalent/non-covalent interactions, reversibility, and native/non-native structure (Cromwell et al., 2006; Philo and Arakawa, 2009). Cromwell et al. (2006) showed that IgG aggregates connect to each other via non-native disulfide bonds between unpaired thiols. Lee et al. (2009) showed that a low ratio of light-chain (LC) mRNA to heavy-chain (HC) mRNA correlates with the amount of IgG aggregates. In fact, it is accepted that the LC is important for IgG folding and assembly in the ER and that cell lines producing a large amount of LC tend to show high productivity and quality (Bhoskar et al., 2013; Ho et al., 2013).

Herein, we aimed to evaluate intracellular IgG aggregates in living cells using AF.2A1, a 25-residue artificial protein that does not bind native IgG conformers but binds efficiently to the Fc region of non-native IgG conformers (Miyafusa et al., 2021; Senga et al., 2017; Senga and Honda, 2018; Watanabe et al., 2014, 2016). To monitor intracellular IgG aggregates in antibody-producing CHO cells, we used an AF.2A1 derivative labeled with a fluorescent marker, fluorescein. Fluorescent-labeled AF.2A1 (AF.2A1-F520) was transfected into CHO cells, which were observed using a fluorescence and confocal microscopy to evaluate the aggregates. The results demonstrated that this method can effectively track the changes in the amount of intracellular IgG aggregates produced in CHO cells. Overcoming the limitations of the conventional methods, our method using live-cell imaging would be useful to minimize aggregation from the early steps of production and improve the production of effective and safe therapeutic antibodies.

RESULTS

In vitro binding of fluorescent-labeled AF.2A1 to non-native IgG conformers

Before the observation of intracellular IgG aggregates in CHO cells, the binding specificity of AF.2A1 to non-native IgG conformers was examined *in vitro*. Native and non-native IgG conformers immobilized on insoluble beads (IgG Sepharose 6 Fast Flow and acid-stressed IgG Sepharose beads, respectively) were used for this experiment. The native or acid-stressed IgG Sepharose beads were mixed with two probes, anti-human IgG antibody DL650 and AF.2A1-F520 for the detection of total IgG and aggregates, respectively, incubated for 1 h, and washed to remove unbounded fluorescent probes; the mixture of anti-human IgG antibody DL650 and fluorescein was used as the negative control. Expectedly, AF.2A1-F520 bound to acid-stressed IgG Sepharose beads, but not to native IgG Sepharose beads (Figures 1A and 1B, lower panels). Meanwhile, fluorescein bound to neither of the beads (Figures 1A and 1B, upper panels) and the anti-human IgG antibody DL650 bound to both beads, validating our experiment (Figures 1A and 1B, right panels). Overall, these results suggest that fluorescence labeling does not interfere with the specific binding of AF.2A1 and that AF.2A1-F520 can distinguish non-native from native IgG conformers.

Next, we examined the difference in fluorescence signals from AF.2A1-F520 bound to large IgG aggregates versus soluble non-native IgG conformers (Figure 2A). After an acid-stressed IgG solution was prepared via dialysis and neutralization as described in the section "METHOD DETAILS," three samples (steps 1, 2, and 3 in Figure 2A) were prepared and observed by fluorescence microscopy (Figures 2B and 2C). Briefly, initial solutions (step 1) containing acid-stressed IgG and AF.2A1-F520 or fluorescein were prepared. After incubation, the solutions were subjected to centrifugation and divided into the supernatant (sup; step 2) and precipitate (ppt; step 3). We found large patches with strong fluorescence in the ppt (Figure 2B, right panel), indicating AF.2A1-F520 bound to large IgG aggregates. Similar patches (with weak fluorescence) were also identified in the initial solution (Figure 2B, middle panel). In contrast, such patches were not observed in the sup portion. In fact, fluorescence images from the sup portion were comparable with those obtained with the solution without the antibody (Figure 2B, left panel). These results suggest that it is difficult to distinguish soluble non-native IgG conformers from native IgG conformers using the fluorescent probe method since AF.2A1-F520 evenly disperses in solution even if it is specifically bound to soluble non-native IgG conformers. Therefore, microscopic imaging using AF.2A1-F520 can be used to detect accumulated non-native IgG conformers, such as large IgG aggregates. Notably, the large IgG aggregates were not detected by fluorescein (Figure 2C).

Live imaging of intracellular IgG aggregates in CHO cells using fluorescent-labeled AF.2A1

We tried to analyze intracellular IgG aggregates in living cells via direct fluorescence imaging using specific fluorescent probes (AF.2A1-F520 and anti-human IgG antibody DL650). Before transfection, we excluded possible accidental interactions between the two probes. Surface plasmon resonance (SPR)

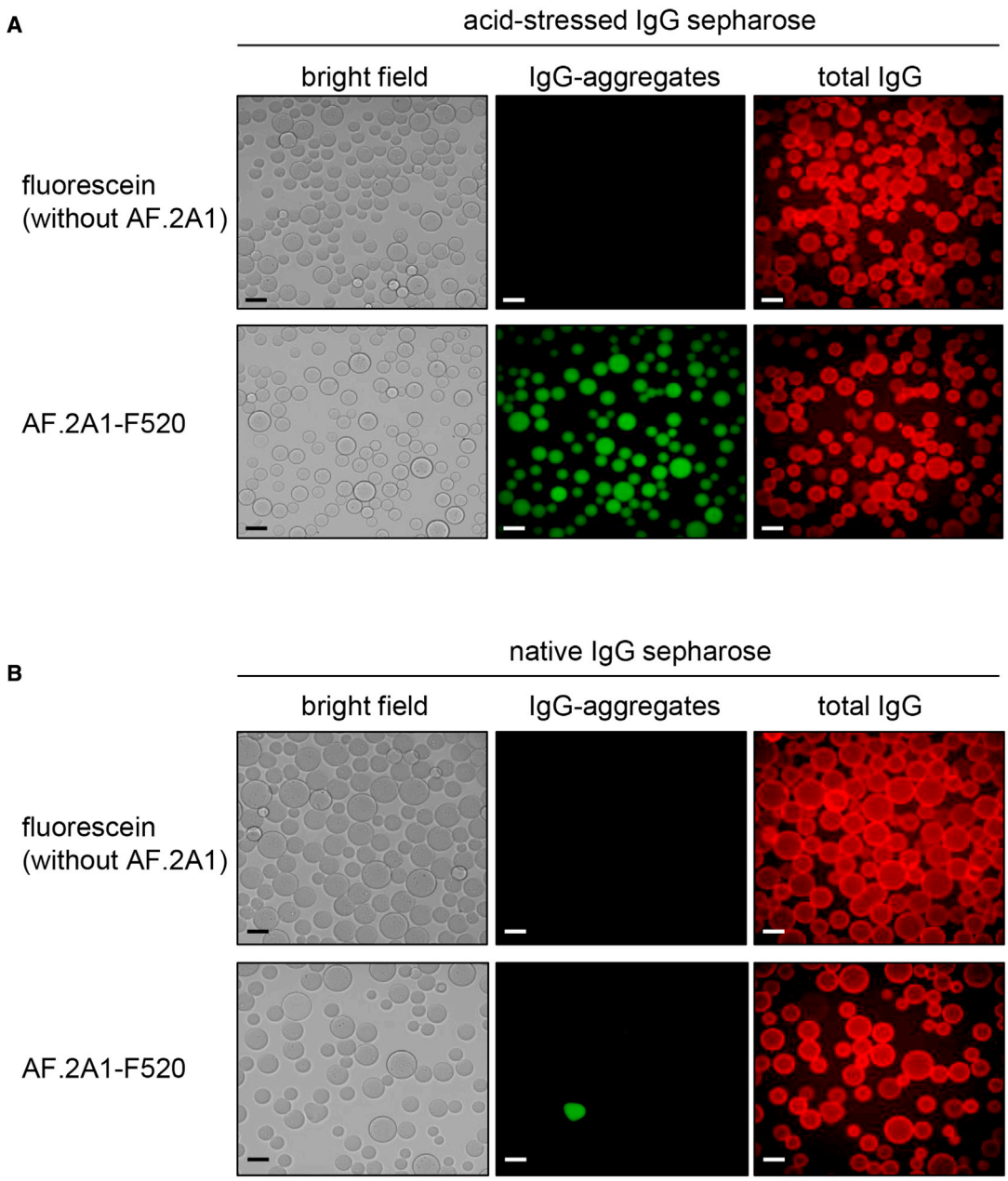

Figure 1. *In vitro* detection of non-native IgG conformers immobilized on beads using fluorescent-labeled AF.2A1

(A) Bright-field and fluorescence micrograph images of acid-stressed IgG Sepharose beads. The beads (50 μL) were incubated with anti-human IgG antibody DL650 (15 nM) and AF.2A1-F520 (15 nM), or anti-human IgG antibody DL650 (15 nM) and fluorescein (15 nM) for 1 h. After a washing step, beads were observed via microscopy.

(B) Bright-field and fluorescence micrograph images of native IgG Sepharose beads. The same procedure as above was followed. Scale bars represent 100 μm.

experiments showed that AF.2A1 does not interact significantly with the anti-human IgG antibody DL650 compared with acid-treated therapeutic IgG (Figure S1), indicating that the chance of interference in CHO cells is small.

Fluorescent micrograph images of CHO-IgG1 cells co-transfected with AF.2A1-F520 and anti-human IgG antibody DL650 are shown in Figure 3A, while those for fluorescein and anti-human IgG antibody DL650 are shown in Figure 3B. Nuclear staining was performed using Hoechst 33342 18 h after co-transfection, followed by analysis using a confocal laser-scanning microscope. In the case of AF.2A1-F520, green patches with strong fluorescence similar to that found in the *in vitro* observation were observed in the antibody-producing CHO cells (Figure 2B, right panel, and Figure 3A, middle panel), suggesting the formation of large IgG aggregates in CHO cells with diameters between several hundred nanometers and 2 μm. Interestingly, the location of the green patches within the cells was not completely similar to that of the red fluorescence produced by the anti-human IgG

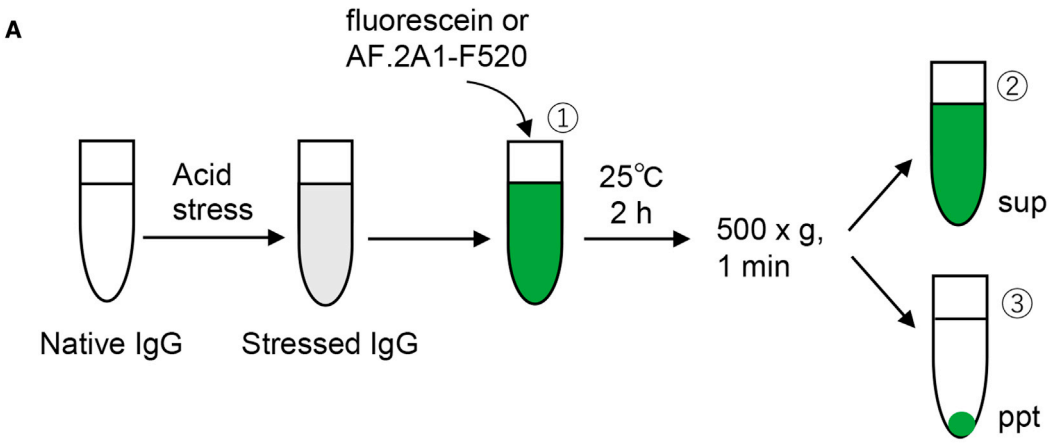

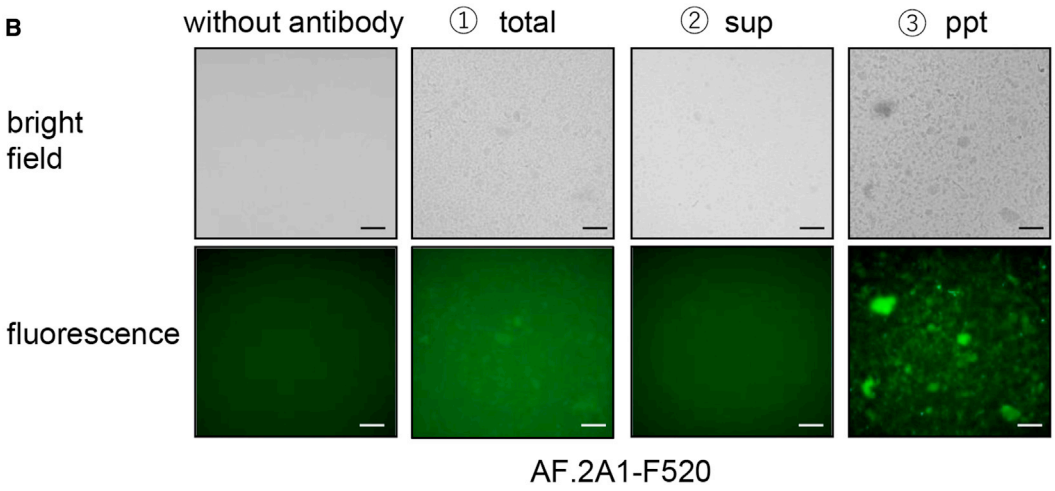

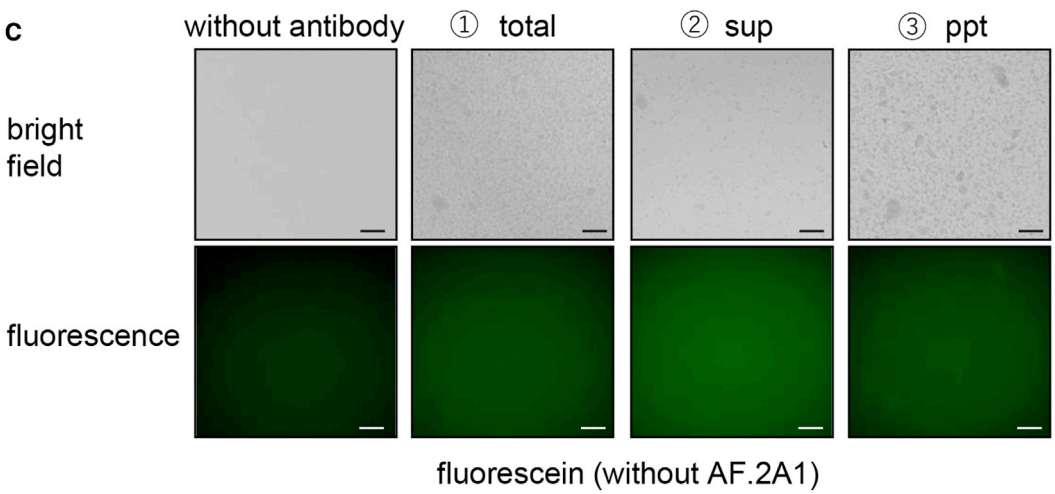

(legend on next page)

antibody DL650. Of note, in the case of CHO-K1 cells (mock cell), such green patches and red fluorescence were not observed in the cells (Figure S2). Hence, we inferred that AF.2A1-F520 specifically binds to aggregates comprising non-native IgG conformers while the anti-human IgG antibody DL650 binds to all of the recombinant IgG produced in the cell regardless of the conformation. In contrast, fluorescein did not show such defined patches (Figure 3B, middle panel). Notably, no significant differences in cell morphology were observed in bright-field observations before or after transfection.

Subsequently, to confirm the co-localization of the two fluorescent probes in the cells, suggested in the above section, we used Förster resonance energy transfer (FRET) microscopy. In the FRET experiment, AF.2A1-F520 and the anti-human IgG antibody DL650 were used as the donor and acceptor, respectively. Bright red patches from the acceptor indicating FRET were observed in CHO-IgG1 cells (Figure 4A, right panels), whereas such red patches were not found in control cells incubated with fluorescein (the control donor; Figure 4B, right panels). Importantly, in line with the above results, the location of bright red patches was completely matched with that of the green patches, indicating IgG aggregates, while, in contrast, not all red patches excited by a 640-nm light indicating total IgG exhibited FRET signals (Figure 4A). Therefore, we further analyzed the FRET performance of individual patches within two different categories: patches emitting strong green fluorescence and patches emitting weak or no green fluorescence. Relative fluorescence intensity (Ex488/Ex640), corresponding to the ratio of the fluorescence intensity when exited at 488 nm to that at 640 nm, was obviously higher for the strong green patches (Figure 4C). Altogether, these results prove the co-localization of AF.2A1-F520 and the anti-human IgG antibody DL650 on a common target, intracellular aggregates comprising non-native IgG conformers, in CHO cells.

Next, the time-dependent dynamics of intracellular IgG aggregation was monitored. Time-lapse observations of living CHO-IgG1 cells transfected with AF.2A1-F520 alone showed that aggregated particles gradually grew to a maximum size (approximately 2–3 μm in diameter) within 90 min once aggregation began and remained in the cell for a considerable amount of time (Figure 5A). Further observations showed faster dynamics of these large particles, with some of them emerging or expanding within a short period, while others disappeared or shrank (Figures 5B, 5C, and S3); these observations were made in the context of CHO cells co-transfected with AF.2A1-F520 and anti-human IgG antibody DL650. Additionally, in the former case, aggregate-containing vesicles were first transported from the cytoplasm to the ER and subsequently to the cell membrane, while, in the latter one, vesicles initially localized around the cell membrane, and then disappeared. We postulate that some of these large aggregate particles are secreted, while others are degraded intracellularly. Generally, newly synthesized, correctly folded proteins are secreted from the ER to the Golgi apparatus, whereas unfolded or misfolded proteins are transferred from the ER to the proteasome and degraded via proteolysis (Haynes et al., 2002; Vembar and Brodsky, 2009). Hence, the gradual growth of aggregates up to micrometer-sized particles suggests that the non-native IgG conformers are not promptly degraded but rather accumulated within vesicles before undergoing intracellular quality control. This is particularly relevant in the context of recombinant protein overexpression in antibody-producing CHO cells.

Estimation of the amount of intracellular IgG aggregates using fluorescent-labeled AF.2A1

If most intracellular aggregates are secreted, the amount of extracellular aggregates should correlate with the amount of intracellular aggregates. Therefore, next, we attempted to estimate the amount of intracellular IgG aggregates. Generally, in therapeutic IgG production, aggregates are evaluated after the purification process using a variety of methods, such as SEC and DLS (Den Engelsman et al., 2011; Imamura and Honda, 2016; Senga et al., 2017, 2019). However, these physicochemical methods are not well suited for the analysis of samples collected upstream in the process since the intracellular and extracellular environments are crowded with many components that may interfere with and distort the analytical results. Thus, we speculated that our approach, using a fluorescent probe highly specific for IgG aggregates, could overcome this limitation.

The addition of excess sugar to culture media generally leads to cellular osmotic stress, which may alter the state of recombinant protein expression (Hwang et al., 2011; Onitsuka et al., 2014). Therefore, we analyzed the effect of trehalose addition on the amount of intracellular IgG aggregates via fluorescence imaging of antibody-producing CHO cells. Figures 6A and 6B show representative confocal images of CHO-IgG1 cells cultured in the absence or presence of 100 mM trehalose (516.7–536.7 mOsm/kg), respectively. The total IgG and relative amounts of intracellular IgG aggregates were estimated using the following formulas: ([anti-human IgG antibody DL650 (red) fluorescence intensity]/[the number of cells counted as per the Hoechst 33342 (blue) staining]) and ([AF.2A1-F520 (green) fluorescence intensity)]/[anti-human IgG antibody DL650 (red) fluorescence intensity]), respectively. The total amount of intracellular IgG decreased to half of that in the non-treated condition in the presence of trehalose (Figure 6C), whereas the relative amount of intracellular IgG aggregates appeared to increase (Figure 6D). These results suggest that the osmotic stress induced by the addition of excess trehalose to the culture medium affected IgG expression, in line with the results of previous studies reporting the induction of autophagy or apoptosis, or the reduction in melanin production in response to salt- or sugar-induced hyperosmotic stress (Bin et al., 2014; Han et al., 2010).

Figure 2. *In vitro* detection of large IgG aggregates in solution using fluorescent-labeled AF.2A1

(A) Outline of the method. An acid-stressed IgG solution was filtered through 0.22-μm centrifugal filters and subsequently mixed with AF.2A1-F520 (1 μM) or fluorescein (1 μM) (step 1). The mixed solutions were incubated for 2 h at 25°C and centrifuged at 500 × *g* for 1 min to separate the supernatant (step 2) from the precipitate (step 3). The three samples (step 1, step 2, and step 3) were then transferred onto a 24-well plate and observed via microscopy.

(B) Bright-field and fluorescence micrograph images of the acid-stressed IgG in the presence of AF.2A1-F520.

(C) Bright-field and fluorescence micrograph images of the acid-stressed IgG in the presence of fluorescein. In both cases, the left panels show images without the addition of acid-stressed IgG. Scale bars represent 100 μm.

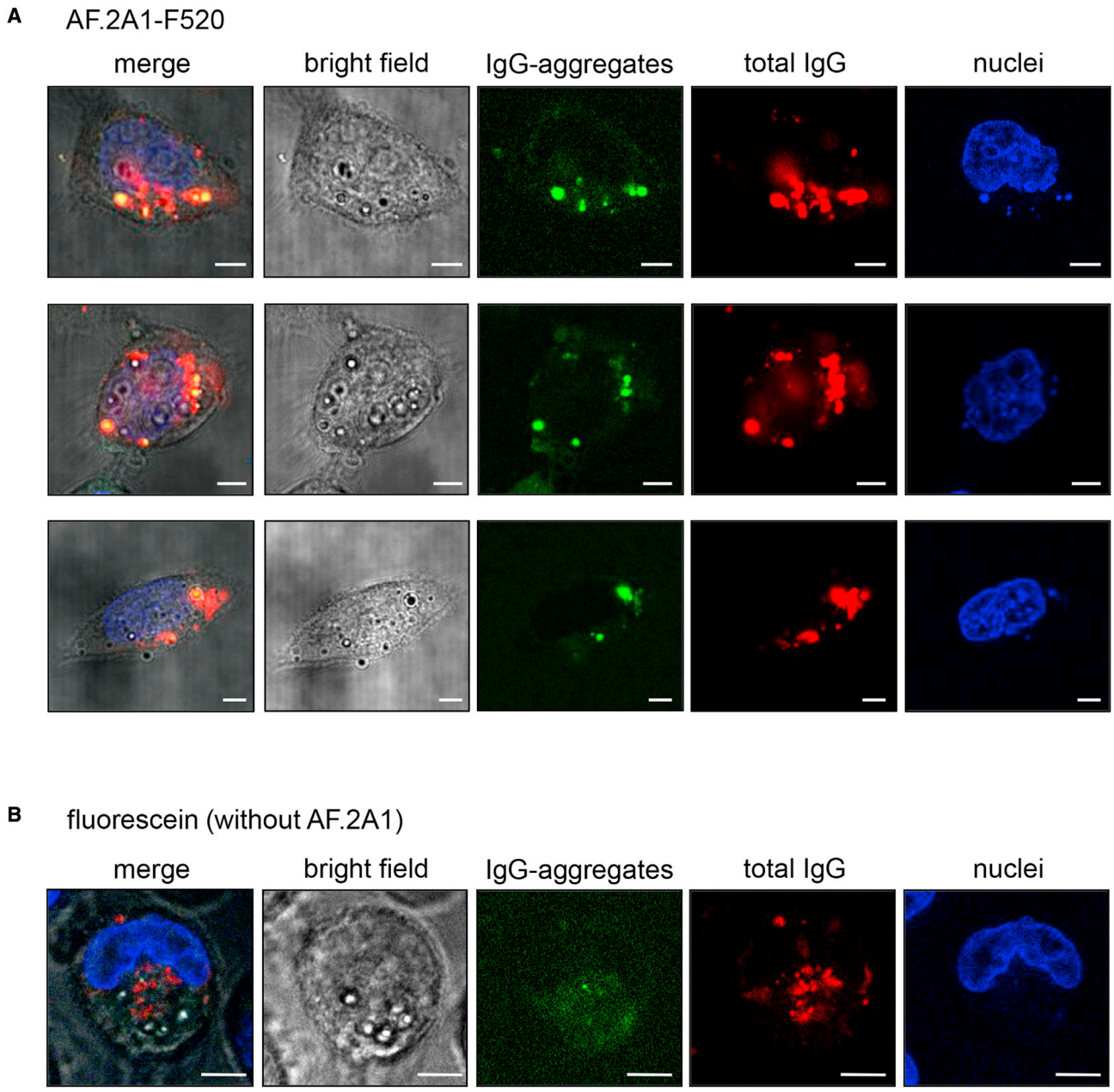

Figure 3. Fluorescence live imaging of intracellular IgG aggregates in CHO-IgG1 cells

(A and B) CHO-IgG1 cells were transfected with 50 ng anti-human IgG antibody DL650 and 2 μg of AF.2A1-F520 (A) or 2 μg of fluorescein (B). After 24 h, nuclear staining was performed, and preparations were visualized under a confocal laser-scanning microscope. Scale bars represent 5 μm.

Lastly, we examined the correlation between the amounts of intracellular and extracellular IgG aggregates. The amount of intracellular IgG aggregates was estimated from fluorescence microscopy images of AF.2A1-F520 and anti-human IgG antibody DL650-stained cells. The amount of extracellular IgG aggregates in purified samples was defined as per the SEC elution profiles. The cell culture supernatant was first purified using protein G + L affinity column chromatography, followed by SEC. In this experiment, we used CHO-IgG3 cells, expressing the difficult-to-express human IgG3 gene (i.e., expression of a protein prone to aggregation). Moreover, trehalose, betaine, trimethylamine *N*-oxide (TMAO), L-Arg, L-Pro, lactitol, sucrose, glycerol, and sorbitol were selected as protecting osmolytes (Street et al., 2006), to raise the free energy of the unfolded state, favoring the folded protein configuration *in vitro*. These osmolytes were added transiently to the culture medium to alter the expression of the antibody and/or the formation of aggregates. Notably, no significant effects were elicited by the additives on the CHO cell culture or IgG3 production (Figure S4). However, an increase in intracellular IgG aggregates was observed in response to

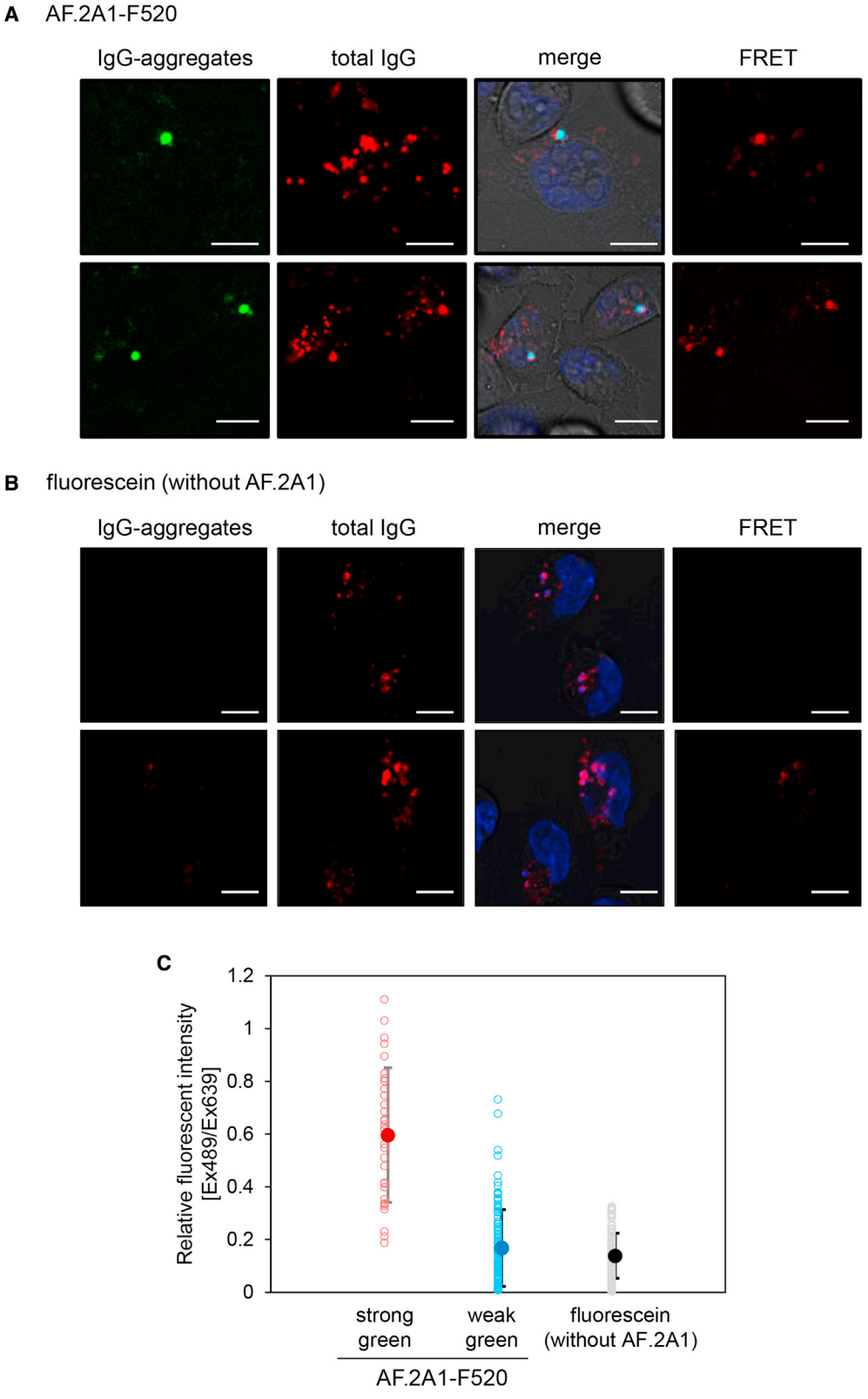

(legend on next page)

trehalose and betaine supplementation, whereas the addition of TMAO, L-Arg, sucrose, and glycerol decreased intracellular IgG aggregates (Figure 7, open bars).

Further, the addition of L-Arg, reported to suppress IgG aggregation *in vitro* (Kheddo et al., 2014), decreased aggregate formation and increased total IgG production in CHO-IgG3 cells (data not shown). Similarly, the amounts of extracellular IgG aggregates changed in the purified samples depending on the additives used (Figures 7 and S5). Protecting osmolytes generally push the folding equilibrium toward the native structure (Street et al., 2006). Herein, we observed an inhibitory effect of various additives on the formation of aggregates, with the exception of trehalose and betaine, which may have induced osmotic stress in the CHO cells. The effects of the additives on the abundance of extracellular IgG aggregates exhibited a similar trend to that observed for intracellular IgG aggregates, suggesting that the intracellular IgG aggregates formed in CHO cells expressing aggregation-prone antibodies directly influence the amount of IgG aggregates in the cell culture supernatants. The incomplete correlation between the abundance of intracellular and extracellular IgG aggregates (Figure S6) may have resulted from some of the intracellular aggregates not being secreted. Alternatively, the intracellular aggregates smaller than a few hundred nanometers in diameter may have been underestimated by confocal microscopy, or the extracellular aggregates larger than the exclusion limit (ca. 1,300 kDa) of the SEC resin may have been excluded from the analysis.

DISCUSSION

In the current study, live-cell imaging of intracellular IgG aggregates in antibody-producing CHO cells was successfully achieved via the use of fluorescent-labeled AF.2A1, a small protein with the ability to bind to non-native IgG conformers with high specificity. The methodological advancements in this study can be summarized as follows. First, labeling AF.2A1 with a fluorescent group at the 12^{th} residual position did not hamper the specific binding of AF.2A1 to non-native IgG conformers; fluorescent-labeled AF.2A1 accumulated in aggregated particles comprising non-native IgG conformers, resulting in the formation of large spots with intense fluorescence. Second, fluorescent-labeled AF.2A1 allowed the observation of the intracellular formation, dynamics, and degradation of aggregates. As shown in Figure 5, fluorescent-labeled AF.2A1 transfected into CHO cells did not degrade promptly; it bound to non-native IgG conformers in the cells, allowing the long-term monitoring of intracellular aggregates. Third, this technology can estimate the relative amount of intracellular IgG aggregates under various culture conditions. The influence of culture additives on the amount of intracellular IgG aggregates, as per the fluorescence intensity of the two probes used, moderately correlated with the effect of these additives on the amount of aggregates in purified antibodies obtained from the culture supernatants. If the amount of antibody aggregates after purification is strongly dependent on intracellular aggregation, the assessment of intracellular IgG aggregates would allow the optimization of expression conditions to minimize aggregates in purified products, thereby decreasing the risk of immunogenicity.

In the culture process using antibody-producing CHO cells, it is estimated that 1%–20% of the total antibodies are present as aggregates in the medium (Gomez et al., 2012). Paul et al. (2014) reported that SEC-based quantification of IgG aggregates can be performed directly in the supernatant of CHO cell cultures without the need for a pre-purification step. Their results demonstrated that the supernatants of CHO cells contained over 75% of IgG dimers and larger oligomers, representing aggregates that may have formed in the cell culture. However, the process of aggregation in the context of cell culture (e.g., when and where such aggregates occur) is not completely understood. A recent study suggested that it is more likely that aggregates are generated in cells and secreted rather than aggregation after antibody secretion (Onitsuka et al., 2019). If this is the case, to explore the mechanism of antibody aggregation, it becomes essential to investigate how differences in culture conditions (e.g., medium composition, temperature, and pH) affect the expression of recombinant proteins in antibody-producing cells; in other words, whether the level of intracellular aggregation changes dynamically, depending on culture conditions. For this purpose, this technology, which can be applied to directly evaluate the formation of intracellular IgG aggregates via live-cell imaging, will be a very effective tool. In addition, evaluation of the amount of intracellular IgG aggregates is expected to offer a new approach for screening antibody-producing CHO cell lines suitable for high-quality production. Moreover, methods to assess intracellular IgG aggregates may help to answer the questions whose answers remain unknown. For instance, which amino acid sequences are prone to intracellular aggregation? Moreover, does aggregation *in vivo* parallel aggregation *in vitro*?

Conventionally, in the production of therapeutic antibodies, conditions are optimized primarily for the purpose of increasing the quantity; however, minimal efforts have been made to reduce the formation of aggregates. For the establishment of stable cell lines, many antibody-producing CHO cells have been screened focusing on productivity-related parameters, such as the amount of antibody produced, proliferation, and passage stability. Furthermore, for the selection of appropriate antibody sequences, the pharmacological function of the antibody is emphasized, while the level of aggregation is rarely considered. Using the fluorescent probe we propose here, it becomes possible to gather the information that has been difficult to obtain

Figure 4. FRET microscopy to detect the co-localization of AF.2A1-F520 and anti-human IgG antibody DL650

(A and B) CHO-IgG1 cells were transfected with 50 ng of anti-human IgG antibody DL650 and 2 μg of AF.2A1-F520 (A) or 2 μg of fluorescein (B). After 24 h, nuclear staining was performed, and the preparations were visualized under a confocal laser-scanning microscope. FRET experiments were performed immediately after the imaging of IgG aggregates, total IgG, and nuclei. Scale bars represent 10 μm.

(C) Comparison of relative fluorescent intensity (Ex488/Ex640), corresponding to the ratio of the fluorescence intensity when exited at 488 nm to that at 640 nm. The FRET performance of individual patches emitting strong green fluorescence, weak fluorescence, or no green fluorescence, and stained with fluorescein alone was analyzed using the ImageJ software; the numbers of patches and cells determined were 31 patches in 13 cells, 166 patches in 13 cells, and 166 patches in 12 cells, respectively. Mean and standard deviations of the intensity of the observed patches are presented.

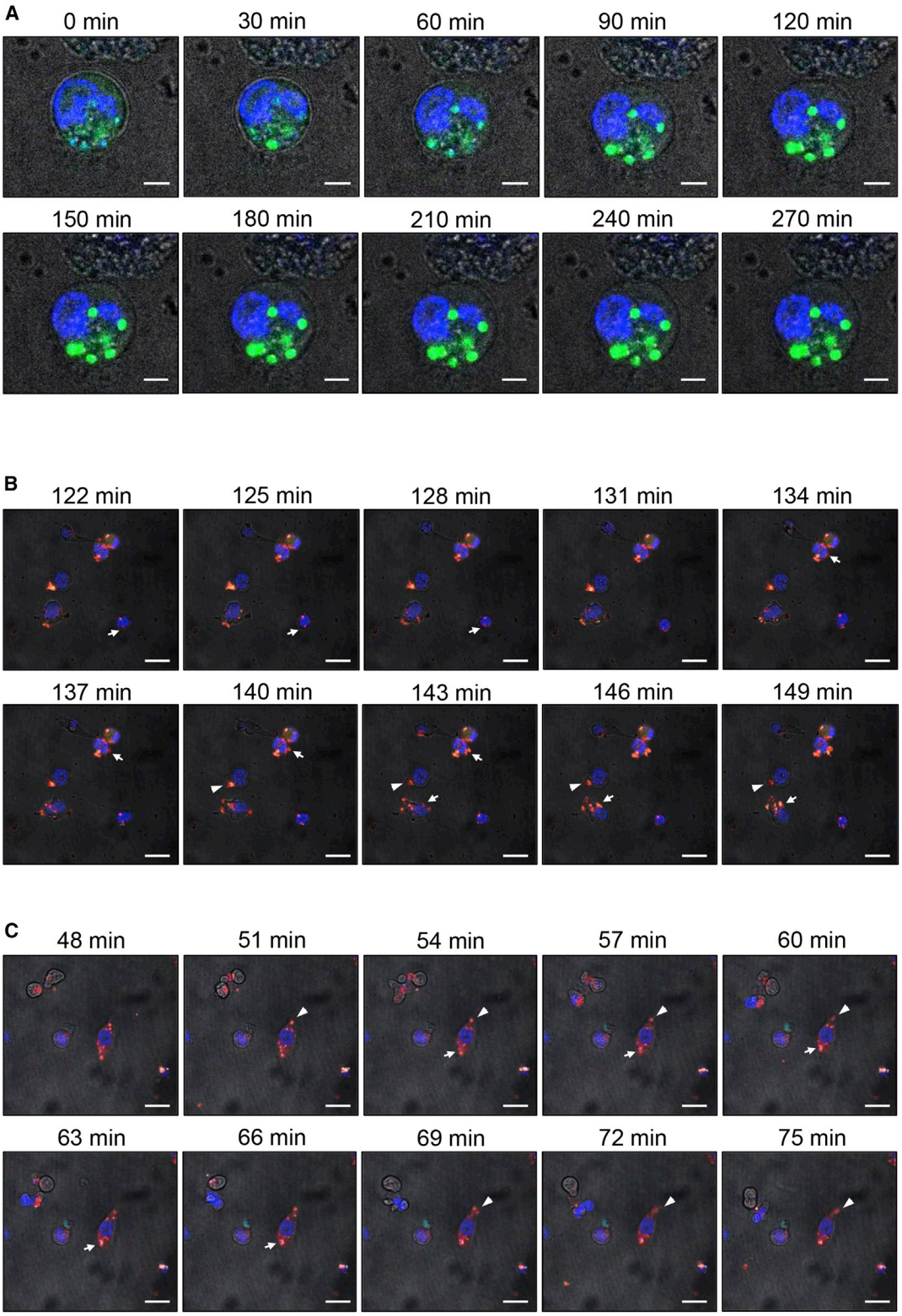

Figure 5. Time-lapse observation of intracellular IgG aggregation in CHO-IgG1 cells using confocal microscopy

(A–C) The observation began 18–20 h after transfection with AF.2A1-F520 (green) and/or anti-human IgG antibody DL650 (red). Scale bars represent 5 μm (A) and 30 μm (B and C). (B and C) The arrows (122–128, 134–143, and 143–149 min in B, and 54–66 min in C) and arrowheads (140–149 min in B, and 51–60 and 69–75 min in C) indicate the emergence and disappearance of large aggregates, respectively.

See for enlarged images in Figure S3.

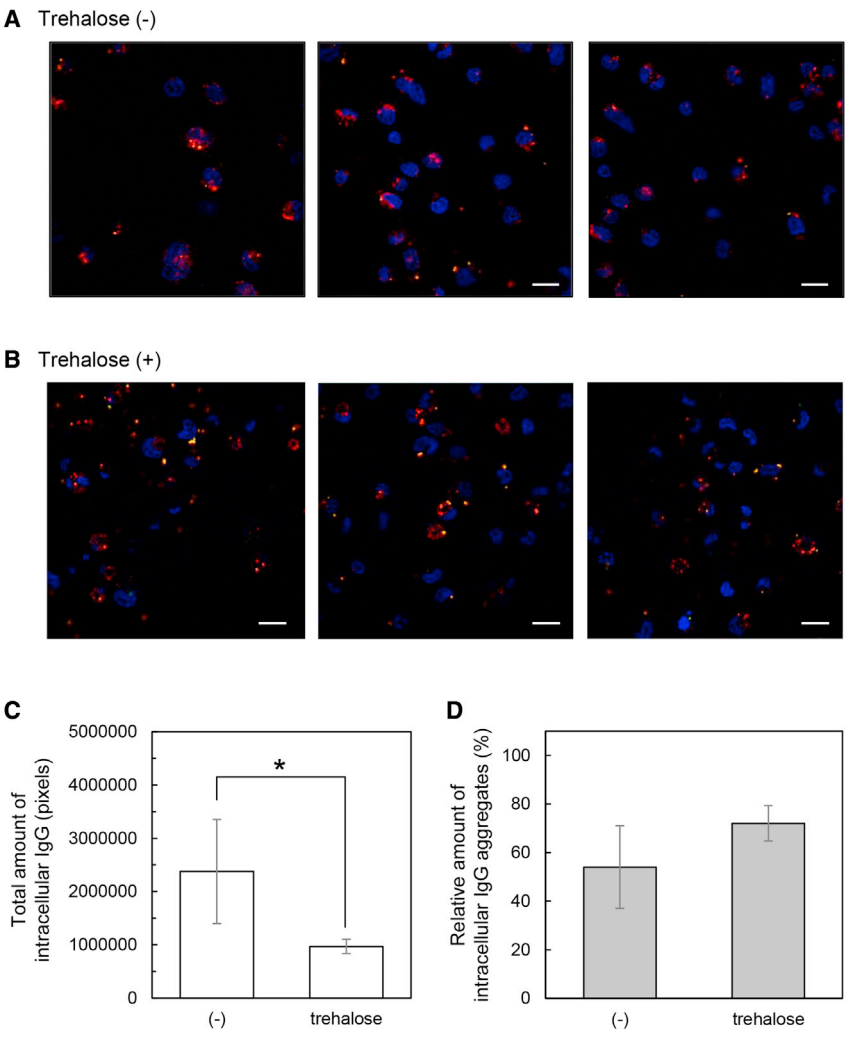

Figure 6. Effect of trehalose treatment on the amount of intracellular IgG aggregates in CHO-IgG1 cells

(A and B) Representative confocal images of CHO-IgG1 cells cultured without (A) or with (B) 100 mM trehalose. Scale bars represent 20 μm.

(C and D) Quantification of the produced IgG presented as the average intensity per cell (C) and the intensity of aggregates' expression (D). Five micrograph images containing 138 cells in total were analyzed in the control condition. Six micrograph images containing 215 cells in total were analyzed in the context of trehalose treatment. Mean and standard deviations of the data of the observed images are presented. Asterisks indicate statistically significant differences (*$p < 0.05$).

with the conventional analysis methods. Hence, this probe will allow for advances toward the high-quality production of antibodies via multiple industrial developments, including the optimization of cell culture conditions, cell line screening, and antibody sequence selection, aiming to minimize the aggregation of therapeutic antibodies.

Herein, we focused on intracellular IgG aggregates and demonstrated the usefulness of live-cell imaging using fluorescent-labeled AF.2A1. Importantly, we expect that this technology will be applicable to the identification of IgG molecules, as well as Fc-fusion proteins that are less prone to aggregate intracellularly. However, some practical challenges remain. Microscopic observation takes a considerable amount of time, which may not be suitable for the live monitoring of an actual culture process. Further improvement in throughput is desired. For instance, replacing confocal microscopy with a high-throughput analysis technique is one possible solution. In addition, the current method based on protein transfection reagents involves complicated steps. Developing simpler and more efficient introduction techniques will be important to facilitate routine analysis at manufacturing sites. Another challenge is to achieve accurate quantification of a small amount of intracellular aggregates. Further developments of this technique are needed, such as preparing a stable reference substance with various particle sizes, validation of the analytical procedure for the live-cell imaging, and enhancing the analytical reliability.

Finally, we emphasize the usefulness of this technology in basic research. Although there are a few reports (Borth et al., 2005; Hooker et al., 1999; Lai et al., 2013; Onitsuka et al., 2019), little is known about recombinant gene expression in antibody-producing CHO cells, especially considering the folding and assembly of translated proteins, post-translational modifications including glycosylation, intracellular quality control, and extracellular secretion. In this study, we found that intracellular IgG aggregates are generated in the cytoplasm and form particles with diameters between a few hundred nanometers and several micrometers; notably, these particles remain in the cytoplasm for a relatively long time without being degraded. These findings suggest that IgG aggregates are secreted intact from the cell to the extracellular milieu, maintaining their size and shape. Russell bodies are known as immunoglobulin-containing inclusion bodies and are usually observed in plasma cells with distended ER. Recently, similar structures to the Russell bodies were also found in antibody-producing mammalian cells, and the relationship between their formation, antibody productivity, and antibody quality has been discussed (Hasegawa et al., 2014). The intracellular IgG aggregates found in this study may have some relation to the Russell bodies, although further characterization is necessary. Importantly, from a methodological point of view, our method has several advantages, such as live-cell imaging, observation of small aggregates down to a few hundred nanometers, and discrimination of aggregates comprising non-native IgG conformers, compared with classical methods used to detect Russell bodies. Therefore, this technology may provide not only a practical tool for the analysis of high-quality antibody production but also for the investigation of the

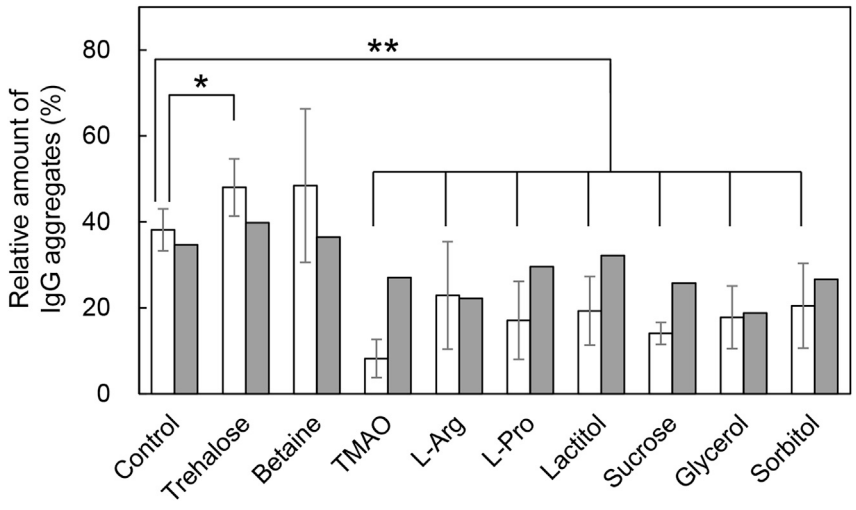

Figure 7. Effects of various additives on the amount of intracellular and extracellular IgG aggregates in CHO-IgG3 cells

The relative amounts of aggregates were normalized to the total amount of IgG. The open bars refer to intracellular IgG aggregates estimated from fluorescence microscopy images in the context of AF.2A1-F520 staining. The closed bars refer to extracellular IgG aggregates, as per the SEC peak area of IgG aggregates in the purified samples. Three independent experiments were performed. Mean and standard deviations of the data of the observed images are presented. Asterisks indicate statistically significant differences (*$p < 0.05$, **$p < 0.01$). The numbers of micrograph images used in the analysis were 8 (control), 10 (trehalose), 10 (betaine), 12 (TMAO), 14 (L-Arg), 13 (L-Pro), 11 (lactitol), 11 (sucrose), 9 (glycerol), and 18 (sorbitol). The numbers of CHO-IgG3 cells used in the analysis were 205 (control), 216 (trehalose), 219 (betaine), 250 (TMAO), 112 (L-Arg), 167 (L-Pro), 282 (lactitol), 250 (sucrose), 134 (glycerol), and 212 (sorbitol).

mechanisms of IgG aggregate formation, degradation, and secretion in cells. Understanding the intracellular aggregation of recombinant IgG will lead to advances in the biopharmaceutical industry and life sciences.

SIGNIFICANCE

In summary, we developed a method for the monitoring of intracellular IgG aggregates in antibody-producing CHO cells using the artificial small protein, AF.2A1. This technique enabled the analysis of IgG aggregates contained in condensed and unpurified samples such as cells and culture supernatants and the long-term monitoring of intracellular IgG aggregates. Moreover, this method will allow for the estimation of intracellular IgG aggregates in CHO cells in the context of culture media with different compositions. Further, we observed a correlation between the amounts of intracellular and extracellular IgG aggregates using CHO cells expressing aggregation-prone antibodies, suggesting not only that intracellular IgG aggregates under various culture conditions can be estimated by this method but also that aggregates are likely first formed intracellularly and then secreted. The potential industrial applications of the proposed method include assessments of IgG genes through the estimation of intracellular aggregates, clone selection of antibody-producing cells, and optimization of cell culture conditions. This method can be used to minimize protein aggregation right from the early steps of production and contribute to the optimization of the manufacturing of effective and safe therapeutic antibodies.

STAR★METHODS

Detailed methods are provided in the online version of this paper and include the following:

SUPPLEMENTAL INFORMATION

Supplemental information can be found online at https://doi.org/10.1016/j.chembiol.2021.08.010.

AUTHOR CONTRIBUTIONS

Y.S. designed the study, performed the experiments, analyzed the data, and wrote the initial draft of the manuscript. M.D. assisted with the experiments and analyzed the data. M.O. designed and performed the experiments. S.H. designed the study, analyzed the data, and edited the manuscript. All authors contributed to data interpretation and critically reviewed the manuscript. The final version of the manuscript was approved by all authors.

ACKNOWLEDGMENTS

We would like to thank Dr. Takamitsu Miyafusa for his contribution to the preparation of AF.2A1-F520, particularly to the establishment of the preparation method. This work was supported in part by the Japan Society for

the Promotion of Science (grant numbers JP19H03363 [to S.H.] and JP20K15105 [to Y.S.]).

DECLARATION OF INTERESTS

S.H. is the inventor of pending patents referring to the artificial protein. The other authors declare no competing interests. This article does not contain any studies with human or animal subjects.

Received: January 8, 2021
Revised: July 5, 2021
Accepted: August 20, 2021
Published: November 4, 2021

REFERENCES

Arosio, P., Rima, S., Lattuada, M., and Morbidelli, M. (2012). Population balance modeling of antibodies aggregation kinetics. J. Phys. Chem. B *116*, 7066–7075.

Bhoskar, P., Belongia, B., Smith, R., Yoon, S., Carter, T., and Xu, J. (2013). Free light chain content in culture media reflects recombinant monoclonal antibody productivity and quality. Biotechnol. Prog. *29*, 1131–1139.

Bin, B.H., Bhin, J., Yang, S.H., Choi, D.H., Park, K., Shin, D.W., Lee, A.Y., Hwang, D., Cho, E.G., and Lee, T.R. (2014). Hyperosmotic stress reduces melanin production by altering melanosome formation. PLoS One *9*, 1–10.

Borth, N., Mattanovich, D., Kunert, R., and Katinger, H. (2005). Effect of increased expression of protein disulfide isomerase and heavy chain binding protein on antibody secretion in a recombinant CHO cell line. Biotechnol. Prog. *21*, 106–111.

Cromwell, M.E.M., Hilario, E., and Jacobson, F. (2006). Protein aggregation and bioprocessing. AAPS J. *8*, E572–E579.

Dengl, S., Wehmer, M., Hesse, F., Lipsmeier, F., Popp, O., and Lang, K. (2013). Aggregation and chemical modification of monoclonal antibodies under upstream processing conditions. Pharm. Res. *30*, 1380–1399.

Eliceiri, K., Schneider, C.A., Rasband, W.S., and Eliceiri, K.W. (2012). NIH Image to ImageJ : 25 years of image analysis. Nat. Methods *9*, 671–675.

Ellgaard, L., Molinari, M., and Helenius, A. (1999). Setting the standards: quality control in the secretory pathway. Science *286*, 1882–1888.

Den Engelsman, J., Garidel, P., Smulders, R., Koll, H., Smith, B., Bassarab, S., Seidl, A., Hainzl, O., and Jiskoot, W. (2011). Strategies for the assessment of protein aggregates in pharmaceutical biotech product development. Pharm. Res. *28*, 920–933.

European Medicines Agency (2015). Guideline on Immunogenicity Assessment of Biotechnology-Derived Therapeutic Proteins (European Medicines Agency).

Feige, M.J., Hendershot, L.M., Buchner, J., and Place, T. (2010). How antibodies fold HHS public access. Trends Biochem. Sci. *35*, 189–198.

Food and Drug Administration (2014). Guidance for Industry: Immunogenicity Assessment for Therapeutic Protein Products (Food and Drug Administration).

Gomez, N., Subramanian, J., Ouyang, J., Nguyen, M.D.H., Hutchinson, M., Sharma, V.K., Lin, A.A., and Yuk, I.H. (2012). Culture temperature modulates aggregation of recombinant antibody in CHO cells. Biotechnol. Bioeng. *109*, 125–136.

Han, Y.K., Kim, Y.G., Kim, J.Y., and Lee, G.M. (2010). Hyperosmotic stress induces autophagy and apoptosis in recombinant Chinese hamster ovary cell culture. Biotechnol. Bioeng. *105*, 1187–1192.

Hasegawa, H., Woods, C.E., Kinderman, F., He, F., and Lim, A.C. (2014). Russell body phenotype is preferentially induced by IgG mAb clones with high intrinsic condensation propensity: relations between the biosynthetic events in the ER and solution behaviors in vitro. MAbs *6*, 1518–1532.

Haynes, C.M., Caldwell, S., and Cooper, A.A. (2002). An HRD/DER-independent er quality control mechanism involves Rsp5p-dependent ubiquitination and ER-Golgi transport. J. Cell Biol. *158*, 91–101.

Ho, S.C.L., Koh, E.Y.C., van Beers, M., Mueller, M., Wan, C., Teo, G., Song, Z., Tong, Y.W., Bardor, M., and Yang, Y. (2013). Control of IgG LC: HC ratio in stably transfected CHO cells and study of the impact on expression, aggregation, glycosylation and conformational stability. J. Biotechnol. *165*, 157–166.

Honda, S., Yamasaki, K., Sawada, Y., and Morii, H. (2004). 10 residue folded peptide designed by segment statistics. Structure *12*, 1507–1518.

Honda, S., Akiba, T., Kato, Y.S., and Sawada, Y. (2008). Crystal structure of a ten-amino acid protein. J. Am. Chem. Soc. *130*, 15327–15331.

Hooker, A.D., Green, N.H., Baines, A.J., Bull, A.T., Jenkins, N., Strange, P.G., and James, D.C. (1999). Constraints on the transport and glycosylation of recombinant IFN-γ in Chinese hamster ovary and insect cells. Biotechnol. Bioeng. *63*, 559–572.

Hwang, S.J., Jeon, C.J., Cho, S.M., Lee, G.M., and Yoon, S.K. (2011). Effect of chemical chaperone addition on production and aggregation of recombinant flag-tagged COMP-angiopoietin 1 in Chinese hamster ovary cells. Biotechnol. Prog. *27*, 587–591.

Imamura, H., and Honda, S. (2016). Kinetics of antibody aggregation at neutral pH and ambient temperatures triggered by temporal exposure to acid. J. Phys. Chem. B *120*, 9581–9589.

Imamura, H., and Honda, S. (2019). pH-shift stress on antibodies. Methods Enzymol. *622*, 329–345.

Imamura, H., Sasaki, A., and Honda, S. (2017). Fate of a stressed therapeutic antibody tracked by fluorescence correlation spectroscopy: folded monomers survive aggregation. J. Phys. Chem. B *121*, 8085–8093.

Jing, Y., Borys, M., Nayak, S., Egan, S., Qian, Y., Pan, S.H., and Li, Z.J. (2012). Identification of cell culture conditions to control protein aggregation of IgG fusion proteins expressed in Chinese hamster ovary cells. Process. Biochem. *47*, 69–75.

Joubert, M.K., Luo, Q., Nashed-Samuel, Y., Wypych, J., and Narhi, L.O. (2011). Classification and characterization of therapeutic antibody. J. Biol. Chem. *286*, 25118–25133.

Kheddo, P., Tracka, M., Armer, J., Dearman, R.J., Uddin, S., Van Der Walle, C.F., and Golovanov, A.P. (2014). The effect of arginine glutamate on the stability of monoclonal antibodies in solution. Int. J. Pharm. *473*, 126–133.

Kunert, R., and Reinhart, D. (2016). Advances in recombinant antibody manufacturing. Appl. Microbiol. Biotechnol. *100*, 3451–3461.

Lai, T., Yang, Y., and Ng, S.K. (2013). Advances in mammalian cell line development technologies for recombinant protein production. Pharmaceuticals *6*, 579–603.

Lee, C.J., Seth, G., Tsukuda, J., and Hamilton, R.W. (2009). A clone screening method using mRNA levels to determine specific productivity and product quality for monoclonal antibodies. Biotechnol. Bioeng. *102*, 1107–1118.

Lippincott-Schwartz, J., Bonifacino, J.S., Yuan, L.C., and Klausner, R.D. (1988). Degradation from the endoplasmic reticulum: disposing of newly synthesized proteins. Cell *54*, 209–220.

Miyafusa, T., Watanabe, H., and Honda, S. (2021). Local disorder of the C-terminal segment of the heavy chain as a common sign of stressed antibodies evidenced with a peptide affinity probe specific to non-native IgG. Int. J. Biol. Macromol. *182*, 1697–1703.

Onitsuka, M., and Omasa, T. (2015). Rapid evaluation of N-glycosylation status of antibodies with chemiluminescent lectin-binding assay. J. Biosci. Bioeng. *120*, 107–110.

Onitsuka, M., Tatsuzawa, M., Asano, R., Kumagai, I., Shirai, A., Maseda, H., and Omasa, T. (2014). Trehalose suppresses antibody aggregation during the culture of Chinese hamster ovary cells. J. Biosci. Bioeng. *117*, 632–638.

Onitsuka, M., Kadoya, Y., and Omasa, T. (2019). Secretory leakage of IgG1 aggregates from recombinant Chinese hamster ovary cells. J. Biosci. Bioeng. *127*, 752–757.

Patel, A.R., Lau, D., and Liu, J. (2012). Quantification and characterization of micrometer and submicrometer subvisible particles in protein therapeutics by use of a suspended microchannel resonator. Anal. Chem. *84*, 6833–6840.

Paul, A.J., Schwab, K., and Hesse, F. (2014). Direct analysis of mAb aggregates in mammalian cell culture supernatant. BMC Biotechnol. *14*, 1–11.

Paul, A.J., Schwab, K., Prokoph, N., Haas, E., Handrick, R., and Hesse, F. (2015). Fluorescence dye-based detection of mAb aggregates in CHO culture supernatants. Anal. Bioanal. Chem. *407*, 4849–4856.

Philo, J., and Arakawa, T. (2009). Mechanisms of protein aggregation. Curr. Pharm. Biotechnol. *10*, 348–351.

Senga, Y., and Honda, S. (2018). Suppression of aggregation of therapeutic monoclonal antibodies during storage by removal of aggregation precursors using a specific adsorbent of non-native IgG conformers. Bioconjug. Chem. *29*, 3250–3261.

Senga, Y., Imamura, H., Miyafusa, T., Watanabe, H., and Honda, S. (2017). AlphaScreen-based homogeneous assay using a pair of 25-residue artificial proteins for high-throughput analysis of non-native IgG. Sci. Rep. *7*, 12466.

Senga, Y., Imamura, H., Ogura, T., and Honda, S. (2019). In-solution microscopic imaging of fractal aggregates of a stressed therapeutic antibody. Anal. Chem. *91*, 4640–4648.

Street, T.O., Bolen, D.W., and Rose, G.D. (2006). A molecular mechanism for osmolyte-induced protein stability. Proc. Natl. Acad. Sci. U S A *103*, 13997–14002.

Vembar, S.S., and Brodsky, J.L. (2009). One step at a time: endoplasmic reticulum. Nat. Rev. Mol. Cell. Biol. *9*, 944–957.

Watanabe, H., Yageta, S., Imamura, H., and Honda, S. (2016). Biosensing probe for quality control monitoring of the structural integrity of therapeutic antibodies. Anal. Chem. *88*, 10101–10095.

Watanabe, H., Yamasaki, K., and Honda, S. (2014). Tracing primordial protein evolution through structurally guided stepwise segment elongation. J. Biol. Chem. *289*, 3394–3404.

STAR★METHODS

KEY RESOURCES TABLE

REAGENT or RESOURCE	SOURCE	IDENTIFIER
Antibodies		
Goat anti-Human IgG-heavy and light chain cross-adsorbed Antibody DyLight® 650 Conjugated	Bethyl Laboratories	Cat#A80-219D5; RRID: AB_10632532
Chemicals, Peptides, and Recombinant Proteins		
Fluorescent-labeled AF.2A1 (AF.2A1-F520)	This paper	N/A
AF.2A1(R12C)	Bio-Synthesis Inc.	https://pubmed.ncbi.nlm.nih.gov/27700033/
Fluorescein-5-maleimide	Thermo Fisher Scientific	Cat#62245
IgG Sepharose® 6 Fast Flow	GE Healthcare	Cat#17096901
Trehalose	FUJIFILM Wako	Cat#20418451
Betaine	FUJIFILM Wako	Cat#023-10862
Trimethylamine *N*-oxide (TMAO)	FUJIFILM Wako	Cat#351-26023
L-Arg	FUJIFILM Wako	Cat#016-04621
L-Pro	FUJIFILM Wako	Cat#161-04602
Lactitol	FUJIFILM Wako	Cat#120-04092
Sucrose	FUJIFILM Wako	Cat#196-00015
Glycerol	FUJIFILM Wako	Cat#079-00614
Sorbitol	FUJIFILM Wako	Cat#194-03752
Hoechst 33342 solution	DOJINDO	Cat#346-07951
Experimental Models: Cell Lines		
The CHO-K1 cells	ATCC	Cat#CRL-9618
The CHO-IgG1 cell lines	Onitsuka and Omasa (2015)	https://pubmed.ncbi.nlm.nih.gov/25548123/
The CHO-IgG3 cell lines	This paper	N/A
Recombinant DNA		
Mammalian PowerExpress system® vector	Toyobo	Cat#MPH-101, MPH-102, MPL-202
Software and Algorithms		
NIS Elements AR (ver. 5.01.00.)	Nikon	https://www.nikon.com/products/microscope-solutions/lineup/img_soft/nis-elements/
BZ-X viewer (ver. 01.03.01.01.)	Keyence	https://www.keyence.com/ss/products/microscope/bz-x800_research/?search_sl=1
Hybrid cell-count software (ver. 1.4.0.1.)	Keyence	https://www.keyence.com/products/microscope/fluorescence-microscope/bz-x700/models/bz-h4c/?search_sl=1

RESOURCE AVAILABILITY

Lead contact

Further information and requests for resources and reagents should be directed to and will be fulfilled by the lead contact, Shinya Honda (s.honda@aist.go.jp).

Materials availability

AF.2A1, its derivatives, CHO-IgG1, and CHO-IgG3 cell lines used in this paper can be obtained from the lead contact upon contract.

Data and code availability

All data reported in this paper will be shared by the lead contact upon request. This paper does not report original code. Any additional information required to reanalyze the data reported in this paper is available from the lead contact upon request.

EXPERIMENTAL MODEL AND SUBJECT DETAILS

Cell lines

CHO-K1 cell line was obtained from ATCC. Two types of antibody-producing CHO cell lines were developed and used in this study: the CHO-IgG1 (Onitsuka and Omasa, 2015), and the CHO-IgG3 cell lines. CHO-K1, CHO-IgG1, CHO-IgG3 cells were cultured and transfected as described in method details.

METHOD DETAILS

Materials

A human IgG1 monoclonal antibody preparation was chosen as a model IgG molecule. Anti-human IgG-heavy and light chain cross-adsorbed donkey polyclonal antibody conjugated with DyLight® 650 (anti-human IgG antibody-DL650) was purchased from Bethyl Laboratories, Inc. (Montgomery, TX, USA). According to the supplier's description, the anti-human IgG antibody-DL650 is selective for humans (minimum reactivity against bovine, chicken, goat, mouse, rabbit, rat, and sheep antibodies); therefore, we assumed this antibody to be specific to recombinant human antibodies in CHO cells. The fluorescein sodium salt, used as the negative control was purchased from Sigma-Aldrich (Montgomery, MO, USA). The CHO-K1 cell line (ATCC-CRL-9618) was purchased from ATCC (Manassas, Virginia, VA, USA).

AF.2A1

AF.2A1 is a 25-residue artificial protein, designed via the modification of a 10-residue protein, chignolin, the smallest foldable polypeptide reported (Honda et al., 2004, 2008). Using chignolin as the structural support, Watanabe et al. obtained AF.2A1 by means of repetitive cycles of segment elongation and a subsequent functional selection from T7 phage-displayed libraries (Watanabe et al., 2014). AF.2A1 recognizes non-native IgG structures generated under chemical or physical stresses and binds specifically to the Fc region of non-native IgG (Watanabe et al., 2014, 2016). The AF.2A1 recognition of non-native structures can be applied to various types of antibodies, regardless of differences in the sequence of the variable region, animal species, and human IgG subclasses (Miyafusa et al., 2021). In addition to acid treatment, our previous studies (Senga and Honda, 2018; Senga et al., 2017) showed that AF.2A1 was useful for the detection of non-native IgG generated under various other stress conditions (e.g., heating, stirring, reducing, and enzyme digestion).

Fluorescent-labeled AF.2A1 (AF.2A1-F520)

To prepare fluorescent-labeled AF.2A1, we replaced the Arg12 residue of AF.2A1 with a Cys residue. The mutated protein, AF.2A1(R12C), was chemically synthesized by Bio-Synthesis Inc. (Lewisville, TX, USA); its purity was confirmed as > 95%. AF.2A1(R12C) was dissolved into 10 mM CH_3COONa buffer (pH 6.5) containing 5 mM ethylenediaminetetraacetate (EDTA). Using the dye stock solution of 10 mM fluorescein-5-maleimide (Thermo Fisher Scientific, Waltham, MA, USA) in dimethyl sulfoxide, we added 20-fold excess of the dye to the protein solution; of note, the maleimide should react with the Cys residues in the target protein. The labeling reaction was performed in the presence of 5% dimethyl sulfoxide (DMSO) for 2 h at 25°C. The reactants were concentrated using 3K molecular-weight cut-off filters (Merck, Darmstadt, Germany) after removing aggregates via spin-down. Thereafter, the solution was dialyzed three times in phosphate buffer containing 0.005% Tween 20 and 5% DMSO using 3.5K MWCO SnakeSkin Dialysis Tubes (Thermo Fisher Scientific, Waltham, MA, USA). Finally, AF.2A1-F520 was purified using a Superdex peptide 10/300 GL column (GE Healthcare, Chicago, IL, USA) equilibrated with PBST buffer.

Acid-stressed IgG immobilized on sepharose beads

Non-native IgG conformers immobilized on insoluble beads were prepared to use in control experiments via the exposure of IgG Sepharose® 6 Fast Flow (GE Healthcare, Little Chalfont, England) to acid stress. The purchased fresh beads were incubated in 100 mM glycine-HCl (pH 2) for 16 h at 4°C(Imamura and Honda, 2016; Senga et al., 2019). The sepharose beads were neutralized via the addition of 1 volume of 1 M Tris-HCl (pH 8.0) to 5 volumes of acid-stressed IgG sepharose beads. The beads were then washed three times in PBS (137 mM NaCl, 2.7 mM KCl, 1.47 mM KH_2PO_4, and 8 mM $Na_2HPO_4 \cdot 12H_2O$; pH 7.4). The acid-stressed IgG sepharose beads were prepared right before any subsequent experiments.

Acid-stressed IgG

Lyophilized IgG preparations were used as the starting materials. To generate non-native IgG conformers induced by acid stress, 1.2 mg/mL IgG solutions in PBS were dialyzed against 100 mM glycine-HCl (pH 2) using a membrane with a 12–14-kDa cut-off for 16 h at 4°C, as reported elsewhere (Imamura and Honda, 2016, 2019; Senga et al., 2019). The dialyzed solutions were stored at 4°C and neutralized via the addition of 1 volume of 1 M Tris-HCl (pH 8.0) to 5 volumes of acid-stressed IgG. The neutralized solutions were promptly filtered using a centrifugal filter unit with a pore size of 0.22 μm (Merck, Darmstadt, Germany). The solution pH was adjusted to 6.9–7.1 and the IgG concentration was adjusted to 1 mg/mL. The acid-stressed IgG preparations were prepared right before any subsequent experiments. The effect of the acid treatment has been characterized using SEC, DLS/SLS, circular dichroism (CD), fluorescence correlation spectroscopy (FCS), and scanning electron-assisted dielectric microscopy (SE-ADM), as reported in our previous papers (Imamura and Honda, 2016: Imamura et al., 2017: Senga and Honda, 2018: Senga et al., 2019). As typical findings, the acid treatment destroys the β-sheet structure of antibodies, promoting aggregate growth in a time-dependent manner.

CHO cell culture

Two types of antibody-producing CHO cell lines were developed and used in this study: the CHO-IgG1 (Onitsuka and Omasa, 2015), and the CHO-IgG3 cell lines. Briefly, the heavy- and light-chain genes of humanized IgG1 and IgG3 were ligated into the Mammalian PowerExpress system® vector (Toyobo, Otsu, Japan). Suspension-adapted CHO-K1 cells (ATCC CRL-9618) were transfected with the respective vectors and the stable cell lines were established via single colony picking. The CHO-K1 cell line was used as a control cell (not able to produce IgG). Cells were grown in BalanCD® CHO growth A medium (Fujifilm Irvine Scientific, Inc., Santa Ana, CA, USA) containing 1% fetal bovine serum (FBS) (GE Healthcare, Little Chalfont, England) and 2 mM L-glutamine (Fujifilm Wako, Osaka, Japan). Cells were grown at 37°C in a humidified incubator with a 5% CO_2/95% air atmosphere.

For the samples supplied for SEC analysis, CHO-IgG3 cells were cultured in SFM4CHO medium (GE Healthcare) supplemented with serum-free TOp2 medium (Irvine Scientific, Santa Ana, CA, USA). Cells were seeded at 0.3 × 10^6 cells/mL in 500 mL Erlenmeyer flasks (Corning Inc., Corning, NY, USA) and incubated at 37°C and 80% humidity, with shaking at 80 rpm. On day 5, any one of the additives, dissolved in culture medium, was added to the culture to a final concentration of 100 mM. Trehalose, betaine, trimethylamine-N-oxide (TMAO), L-arginine (L-Arg), L-proline (L-Pro), lactitol, sucrose, glycerol, and sorbitol were purchased from Fujifilm Wako Pure Chemical (Osaka, Japan) or Nacalai Tesque (Kyoto, Japan). IgG3 antibodies were purified from culture supernatants on day 9 using a HiTrap Protein G HP-HiTrap Protein L-conjugated column (GE Healthcare). An Arg-HCl solution (1M, pH 4.0) was used as the elution buffer to avoid antibody aggregation caused by low-pH exposure

Transfection of proteins and cell staining

The transfection of AF.2A1-F520 and anti-human IgG antibody-DL650 into CHO-K1, CHO-IgG1, or CHO-IgG3 cells was performed with the help of Ab-DeliverIN (OZ Biosciences, Marseille, France), composed of lipid-based chemicals designed to promote the intracellular delivery of large proteins, such as antibodies, according to the manufacturer's instructions. CHO cells were plated at 0.5 × 10^5 in a 35 mm dish in 200 μL of BalanCD® CHO growth A medium, containing 1% FBS and 2 mM L-glutamine. After 16–20 h of culture, cells were transfected via incubation for 16–18 h in 100 μL of BalanCD® CHO growth A medium, containing 1% FBS, 2 mM L-glutamine, 0.8 μL of Ab-DeliverIN, 50 ng anti-human IgG antibody-DL650, and 2 μg AF.2A1-F520; fluorescein was used as a negative control. After transfection, cells were washed several times with culture medium and kept 18–20 h until further observation. Nuclear staining was performed 1.5 h before observation using the Hoechst 33342 staining dye solution (Abcam, Cambridge, England).

Fluorescence microscopy

The all-in-one fluorescence microscope BZ-X700 (Keyence Co., Osaka, Japan) was used to capture images of IgG sepharose or CHO cells, using the appropriate filter sets. For the *in-vitro* detection of non-native IgG conformers, the exposure time was set in the range of 1/25 to 1/4000 seconds, and the 10× objective lens was used. For the observation of CHO cells, the exposure time was set in the range of 1/2 to 1/3 seconds, and the 40× objective lens was used. The sum of the cell images' fluorescence intensities was quantified using the Hybrid cell-count software (Keyence Co., Osaka, Japan). The mask function installed in the software was selected, followed by setting green and red fluorescence signals with fixed parameters for AF.2A1-F520 and anti-human IgG antibody-DL650, respectively. For the quantification of aggregates in cells treated by various additives, multiple images were automatically examined using the Macro cell-count software (Keyence Co., Osaka, Japan) and the parameters mentioned for the Hybrid cell-count software analysis.

Confocal microscopy

Confocal images were acquired on an inverted confocal microscope (Nikon A1, Nikon Co., Tokyo, Japan) with a 60× objective lens, and were analyzed using the NIS-Elements C/NIS-Elements C-ER software. The images were acquired in the same focal plane of the nucleus. Image acquisition was done at a resolution of 1024 × 1024 pixels. The pinhole was set to 1, and the laser power and the sensitivity of the detector were adjusted while exposing. Two independent images were acquired for the same object and averaged to reduce noise. For the quantification of the fluorescence intensity of AF.2A1-F520 (green) or anti-human IgG antibody-DL650 (red), the same configuration setting was used through the experiments. The intensity was quantified based on the sum of the brightness of pixels per region of interest (ROI) in a single z-axis flame. For the selection of the ROI, the "rectangle" mode was selected and loaded onto the entire image. The Z-stack acquisition was performed in cells transfected with fluorescent probes during time-lapse observation. Time-lapse imaging was done at a resolution of 1024 × 1024 pixels without averaging.

FRET microscopy

FRET microscopy was based on the excitation of a donor molecule (AF.2A1-F520 or fluorescein) at 488 nm using a confocal microscope and detecting the emission by an acceptor molecule (anti-human IgG antibody-DL650) at 700 nm. For reference, the images of IgG-aggregates and total IgG were also obtained for the same samples by measuring the 525 nm-emission from AF.2A1-F520 excited at 488 nm and the 700nm-emission from anti-human IgG antibody-DL650 excited at 640 nm. These images were analyzed using the ImageJ (version 1.50i) software, an image-manipulation program developed by the National Institutes of Health (Eliceiri et al., 2012). The FRET performance was expressed as the relative fluorescent intensity [Ex488/Ex640] ([fluorescence intensity from the acceptor by exciting the donor at 488 nm)] / [fluorescence intensity from anti-human IgG antibody-DL650 directly excited at 640 nm]).

Surface plasmon resonance (SPR)

SPR was performed using a Biacore T100 (GE Healthcare). Before measurements, 9533 RU of AF.2A1 were immobilized on a Series S sensor chip CM5 (GE Healthcare). The reference cell was blocked with 1 M ethanolamine. Binding assays were performed under HBS-T (10 mM HEPES (pH 7.4), 150 mM NaCl, 0.005% (w/v) Tween 20). To determine if AF.2A1 shows non-specific interactions with the anti-human IgG antibody-DL650, the antibody was examined using SPR. Native therapeutic IgG and acid-treated therapeutic IgG were also examined as negative and positive controls, respectively. Acid-treated IgG was prepared via the dialysis of human monoclonal IgG against 20 mM sodium acetate (pH 2.0). Data were processed using the Biacore T100 evaluation software (GE Healthcare).

Size exclusion chromatography (SEC)

Purified IgG3 including light chain was analyzed via SEC using a Superdex 200 column (GE healthcare). Aliquots of the protein solution (500 μL) were loaded onto the column and eluted at a flow rate of 0.5 mL/min, with a buffer containing 20 mmol/L phosphate buffer solution (pH 7.0) (Nacalai Tesque, Kyoto, Japan). The ultraviolet absorption signal of the eluate was monitored at 280 nm. The SEC peak profiles were analyzed using the multi-peak fitting function of the IgorPro software (WaveMetrics Inc., Portland, OR) to estimate the relative contents of IgG3 aggregates.

QUANTIFICATION AND STATISTICAL ANALYSIS

Statistical analysis

All data were collected from more than eight images. Statistical analysis was carried out using Microsoft Excel software; statistical significance was investigated using the Student's t-test. Statistical significance was set at $p < 0.05$. Data shown in figures are representative results of individual experiments. p values were stated in the figure legends. Sample size and statistical tests are also reported in the figure legends.